ICMIEE22-096

Comparative Study on Turbulence Modeling of Blood Flow in Flexible Walled Stenosed Artery

Md Sartaj Ahamed Rifath[1], Ahmed Abrar Shayor[2,*], Abdullah Al-Faruk [3]
[1] Department of Mechanical Engineering, Khulna University of Engineering & Technology, Khulna-9203, BANGLADESH
[2] Department of Mechanical Engineering, Khulna University of Engineering & Technology, Khulna-9203, BANGLADESH
[3] Department of Mechanical Engineering, Khulna University of Engineering & Technology, Khulna-9203, BANGLADESH

ABSTRACT
Cardiac diseases are considered as major cause of mortality and disability in the modern world. Prediction of the effect of blockage in the blood flow inside the artery could help us to reduce the death rate due to those diseases. Using biomechanics, the result of blockage in the artery can be predicted. Several turbulence models have been introduced to predict the fluid flow in this field. Numerical simulations have been done before using laminar, turbulent flow, rigid wall, flexible wall combinations. But the main drive for this investigation was finding cases specifically for a case involving 50% stenosis and incorporating physics of wall, blood and turbulence models to provide new insight to such a new case study. Imbibing the concepts from literature review, the shift from laminar to turbulence and the result of a turbulent flow was analyzed using four turbulence models (Realizable K-ε, RNG k-ϵ, Standard k-ω, and SST k-ω flexible artery walls. Properties of artery wall was taken considering the artery as linear elastic material. Flow of blood through stenosed artery causes velocity and pressure change from a normally uniform flow to non-uniform flow. Due to pressure gradient, there was deformation leading to corresponding pressure, velocity changes again. To solve this two-way fluid solid interaction (FSI), system coupling is used with the aid of ANSYS software. The FSI additional parameter would embellish the numerical results done by peers in this field specially using different turbulence models. Velocity, pressure, streamline and wall shear stress (WSS) were the variables used to analyze the case. Since turbulence model change causes mainly significant changes in WSS the one giving closer WS values in contrast to previous validated simulations was selected as the better turbulence model in the range of Re=1000 in this inquest. It seems that standard k-ω SST model can predict the better behavior of flow characteristics due to the effect of wall shear in stenosed artery.

Keywords: Turbulence Models, Steady Flow, Flexible walled artery, CFD, Stenosis

1. Introduction

Atherosclerosis is a prevalent aortic disease that harms scores of people throughout the globe, left untreated can lead to. Plaques form when cholesterol builds up in an artery wall and connective tissue proliferates, causing it to grow inward and limit blood flow. This flow pattern may stimulate continued and possibly more aggressive progression of the stenosis once the vascular constriction or stenosis becomes severe enough to generate a flow separation zone. Moderate and severe stenoses might cause a flow disturbance downstream of the stenosis. Based on rate of flow through stenosis and the shape of the constriction, these perturbed flows may remain laminar or convert to a chaotic, turbulent one. Because turbulence indicates an aberrant flow condition in the circulation, the emergence of turbulent flow has significant therapeutic implications.

Diagnostic tools bolstering MRI and Doppler Ultrasound in-vivo techniques are frequently used to assist the surgeon in making treatment decisions. CFD techniques, on the other hand, can be used to assess blood flow patterns when combined with medical pictures. The CFD method greatly aids in finding locations of flow separation and recirculation, resulting in lower else variable wall shear stresses that aggravate plaque growth and may as well play a key part in plaque rupture. Biomechanics can have a significant impact on the examination of the causes of atherosclerotic artery disease.

Wood et al. [13] discovered that SST k-ω model shows a clear benefit over the regular k- ω model but still warrants more testing of these two model for various Reynolds numbers and pulsatile flow circumstances. Highly simplified case with steady state, 2D model having smooth contours, flexible wall was studied in this exploratory work. Reza et al. [14] research has concentrated intensely on a novel method in which at the beginning of turbulence to the laminarization zone, the modelling using turbulent (k– SST Transitional) flow was used, and with the initiation of the laminarization district, the laminar model was used again using FLUENT to simulate stenotic flows incorporating 50 and 75 percent reduced cross-sectional area and Reynolds numbers going from 500 up to 2000. (v6.3.17). The flow was implicated to be axisymmetric, time independent.

The results obtained by Farzan Ghalichi et al. [15] with low-*Re* turbulence model results were matched with experimental measurements along with the standard *k-ϵ* model obtained results. Thus, showcasing that low-*Re* model predicted results are in sound agreement with the experimental findings.

The fluid-structure interaction flow of viscoelastic blood flow with artery wall is analyzed using ANSYS 16.2 simulation software, and the consequent wall deformation was recorded in the study of Kallekar et al. [16]. For constant flow in the artery, a comparison of wall deformation utilizing flexibility models such as Rigid, Linear Elastic, Neo-Hookean, Mooney-Rivlin, and Holzapfel was produced. The maximal wall displacement anticipated by the Holzapfel model in coronary flow circumstances is only about half of what the Neo-Hookean model predicts. The dimensional changes that were flow-induced reported here with a physiologically appropriate

* Corresponding author. Tel.: +88-01627285545
E-mail addresses: ahmadshayor963@gmail.com
: alfaruk.bd@gmail.com

model for a patient-derived stenosed coronary artery are the first of their kind. These findings are quite useful in angioplasty planning.

Rahman1 et al. [17] investigated various parameters of blood for the simulation. The Reynolds number for this investigation ranges from 96 to 800, low-Re *k-ω* was implemented. The research was done to characterize two non-Newtonian blood constitutive equations, namely (i) the Carreau and (ii) the Cross models along with Newtonian viscosity model. The Newtonian model's outcomes were compared to those of non-Newtonian models. At the pre-stenotic, throat, and soon downstream to throat areas at early systole, pressure and wall shear stress (WSS) discrepancies between Newtonian and other models are visible.

In the Jahangiri et al. [18] conducted investigation of unsteady blood flow in flexible coronary artery having 80% constriction by using ADINA software..K-ε Standard and K-ε RNG used and put head-to-head. K-ε Standard model have a better agreement with laboratory results demonstrating changes that arise by from using flexible wall instead of stiff wall and laminar flow to turbulent flow. Also, assumption of laminar flow in comparing with turbulent flow show less circumferential stress for artery wall. Another result is that in both cases flexibility of wall leads to the reduction of shear stress oscillation. Difference between rigid and flexible wall shear stress in assumption of turbulent flow is higher than assumption of laminar flow [18]. In the study of Tan et al. [19] researchers used newly constructed two-equation models that are for transitional and turbulence scenarios to predict blood flow nature where plaque formation, progression, and shape at rupture are all influenced by low and fluctuating WSS. The transitional version of SST was discovered to have greater overall agreement with empirical results for pulsatile flow in an axisymmetric stenosed tube (patient-specific geometry) simulation results. Using patient-specific boundary conditions, a magnetic-resonance (MR) graphics model of the arteries(carotid) ,70% blocked, study was done and when deviations in the WSS occurred, the laminar flow hypothesis was shown to be unsatisfactory.

Selmi et al. [20] investigated the behavior of the vessel walls using the neo-Hookean hyperplastic model. The distributions of velocity, pressure and deformations were studied.

The existing literatures have deliberated the stenosed artery instance form different perspectives of applying multiple turbulence models with rigid wall consideration or laminar flows and any single turbulence model with flexible wall assumptions. However, an investigation of different turbulence model while employing a compliant vascular wall model has not been carried out. This research might put new insight into this field as when deformable, the near wall assumptions for each model should give slight, but still significant, variations in shear stress and other hemodynamic study parameters. This is because k-ε models (RNG & Realizable) apply wall functions and for complex geometry and flow separation they do very good. While k-ω and k-ω SST model has blending function applied with limiters. Also, this study will aid future researchers in selecting a better turbulence model for advanced simulation in the biomechanics field ultimately aiding in the prediction of additional plaque formation owing to stenosis, lowering the rate of death from cardiac arrest and stroke.

2.Theory

Low-Re, Standard, RNG (Renormalization Group), and Realizable are all different types of *k-ε*. All of these models use transport equations for describing the key variables-dissipation rate (ε) and turbulent kinetic energy (k).

The Reynolds stress in the RANS equation needs to be modeled to solve the equation:

$$\frac{\partial(\rho u_i)}{\partial t}+\frac{\partial(\rho u_i u_j)}{\partial x_i}=-\frac{\partial p}{\partial x_i}+\frac{\partial}{\partial x_j}\left[\mu\left(\frac{\partial u_i}{\partial x_j}+\frac{\partial u_j}{\partial x_i}-\frac{2}{3}\delta_{ij}\left(\frac{\partial u_l}{\partial x_l}\right)\right)\right]+\frac{\partial}{\partial t}(-\rho\overline{u_i u_j}) \quad (1)$$

where Reynolds Stress Tensor,

$$\left(-\rho\overline{u_i u_j}\right)=\mu_t\left(\frac{\partial u_i}{\partial x_j}+\frac{\partial u_j}{\partial x_i}\right)-\frac{2}{3}(\rho k+\mu_t\frac{\partial u_k}{\partial x_k}) \quad (2)$$

$$\mu_t=C_\mu\frac{\rho k^2}{\epsilon} \quad (3)$$

k stands for turbulence kinetic energy, ϵ for dissipation of kinetic energy.

Transport equation for k:

$$\frac{\partial(\rho k)}{\partial t}+\nabla.(\rho U k)=\nabla.\left[\left(\mu+\frac{\mu_t}{\sigma_k}\right)\nabla k\right]+P_k+P_b-\rho\epsilon+S_k \quad (4)$$

P_k stands for production due to mean velocity shear, P_b for production due to buoyancy, while S_k for user defined source.

The transport equation for k is common for RNG, realizable and standard *k-ϵ* model.

<u>k-ϵ Model</u>

The transport equation for ϵ :

$$\frac{\partial(\rho\epsilon)}{\partial t}+\nabla.(\rho U k)=\nabla.\left[\left(\mu+\frac{\mu_t}{\sigma_\epsilon}\right)\nabla\epsilon\right]+C_1\frac{\epsilon}{k}(P_k+C_3P_b)-C_2\rho\frac{\epsilon^2}{k}+S_\epsilon \quad (5)$$

For Realizable k-ϵ model, $C_2=1.9$

For RNG k-ϵ model $C_1=1.42$, $C_2=1.68$

<u>k-ω Model</u>

Actually, evolution of *K-ω* model is from *k-ϵ* model. The only difference lies in the dissipation rate.

The transport equation for k:

$$\frac{\partial(\rho k)}{\partial t}+\nabla.(\rho U k)=\nabla.\left[\left(\mu+\frac{\mu_t}{\sigma_k}\right)\nabla k\right]+P_k+P_b-\rho\epsilon+S_k \quad (6)$$

The transport equation for ω :

$$\frac{\partial(\rho\omega)}{\partial t}+\nabla.(\rho U\omega)=\nabla.\left[\left(\mu+\frac{\mu_t}{\sigma_\epsilon}\right)\nabla\omega\right]+\frac{\gamma}{v_t}P_k-\beta\rho\omega^2$$

Here,

$$\omega=\frac{\epsilon}{C_\mu k} \qquad C_\mu=0.09$$

<u>k-ω SST Model</u>

The transport equation for *K-ω* SST model comes:

$$\frac{\partial(\rho k)}{\partial t}+\nabla.(\rho U k)=\nabla.\left[\left(\mu+\frac{\mu_t}{\sigma_k}\right)\nabla k\right]+P_k+P_b-\rho\epsilon+S_k \quad (7)$$

$$\frac{\partial(\rho\omega)}{\partial t} + \nabla.(\rho U\omega) = \nabla.\left[\left(\mu + \frac{\mu_t}{\sigma_k}\right)\nabla\omega\right] + \frac{\gamma}{v_t}P_k - \beta\rho\omega^2 + 2\frac{\rho\sigma_{\omega 2}}{\omega}\nabla k:\nabla\omega \quad (8)$$

Adjacent to the wall, F_1=1 (K-ω model)
Far from the wall, F_1=0 (k-ϵ model)
So, the blending function depends on the distance of near wall.

$$\mu_t = \frac{a_1\rho k}{\max(a_1\omega, SF_2)} \quad (9)$$

In the model for SST a limiter of viscosity is added. If F_2 or S has high value,then the value of viscosity is small**.**

3. Numerical Modelling

The Numerical Methodology including the geometry creation,meshing,solution of flow physics using accurate options in the solver are as follows.

3.1 Geometry

The stenoses have the following geometry, which is identical to the experimental models as in Eq(1)

$$\frac{r(z)}{D} = 0.5 - A\left[1 + cos\pi\frac{z}{D}\right] \quad (10)$$

Where A=.073 for 50% stenosis constriction, -D ≤ z ≤ D here Z = 0 at the middle of the stenosis), D - normal artery diameter (in the above geometry, 1 cm), and r(z) - local radius that changes with axial distance along z. The level of stenosis is calculated as [1- (r/R)^2], where r and R are the neck and unstenosed, normal arterial radii, respectively. The length of the pre-stenosed region is 50mm, post-stenosed region is 150 mm. The total range of stenosed region is 20mm.
50 % stenosis was chosen and employed here simply to compare with existing literature [8] with similar assumptions. One fact is here focus on non-critical stenosis, transitional stage condition (< 60%) and another is in [8] they have more confidence in 50 % stenosis corresponding results to be more accurate as a low-Re model was used there.

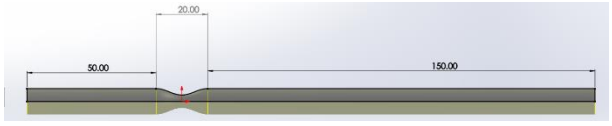

Fig.1 Dimension of a 3D artery fluid zone (mm)

Fig.2 3D outer view of an artery wall

3.2 Blood and Blood Properties:

Blood is a viscoplastic fluid [23]. To make the analysis easier the following suppositions were made to simplify the analysis: (1) With a fixed kinematic viscosity and mass density as mentioned in **Table 1** , the fluid (blood) is considered homogeneous, incompressible, and Newtonian (2) The flow is steady and constant. For big arteries, the steady flow assumption is reasonable [8] since diastole, which lasts about two-thirds of the cardiac cycle, has a reasonably constant forward flow.

Table 1: Blood Properties

Density (Kg/m^3)	1050
Viscosity (Pa.sec)	.0033

.

3.3 Flexible Wall and Properties

Arteries walls are predominantly anisotropic non-linear elastic. Since we are actually dealing with muscular arteries here (distributing arteries). Few researches have employed such representational models of arteries for modeling blood flow; Instead, most studies have used approximations for the arterial wall, such as thin-shell [3], Linear Elastic model [4], Neo-Hookean [5], Mooney-Rivlin model [6], or modified Mooney-Rivlin model [7]. For the sake of simplicity, the wall properties are assumed to be linear elastic. The properties are:

Table 2: Artery wall properties

Thickness of artery wall (m)	.001
Elasticity modulus of the vessel wall (KPa)	910
Density of artery wall (Kg/m^3)	1300
Poisson ratio of vessel wall	.49

3.4 Mesh

GAMBIT v2.4.6 (ANSYS) was used to accomplish the geometry and mesh creation for the model in this research. Quad-Map approach (Quadrilateral elements) was applied. Because the simulation results must be mesh independent, several different element sizes were created and applied in this study. For desirable results, the flow analysis required $y_p\sqrt{U/vz} \leq 1$ (ANSYS FLUENT v6.3.17) and $y^+ \leq 1$ where y_p means the distance to the wall from the next cell centroid, while U the mean velocity. Elements size was taken 0.5 mm for the whole body. Multizone was applied using method. Inflation was applied outer contract region of the fluid zone.

Fig.3 3D meshed stenosed fluid zone (blood)

Artery wall was meshed in the static structure. Elements size was taken 1mm. Face meshing was applied at the inlet and outlet surfaces of the artery wall and body. Total number of nodes and elements were 55300 & 7875.

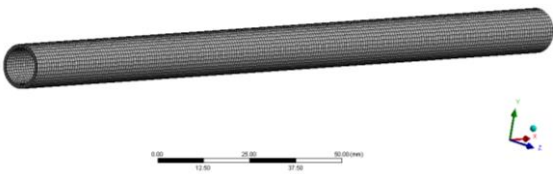

Fig.4 Meshed 3D artery wall outside view

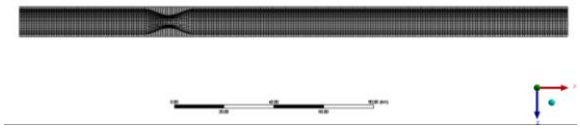

Fig.5 Meshed 3D artery wall inside view

Table 3 Historical data of vapor pressure of ammonia.

Author	Year	*T*	*p*	Ref.
Keyes	1918	240-398	0.103-9.96	1
Cragoe	1920	195-343	0.00563-3.31	25
McKelvey	1923	195-195	0.1	26
Beattie	1930	303-405	1.17-11.3	8
Overstreet	1937	176-242	0.0008-0.1114	27

3.5 Solver Settings

ANSYS CFX 19.2 was used to model using two domains, namely, blood and the artery. To simulate the artery wall portion ANSYS Static Structure module was used. A file named "artery" was created in engineering library and the material properties like density, bulk modulus, elastic modulus, and Poisson's ratio was given. For solving blood section ANSYS FLUENT was used. Turbulence model, blood properties and boundary conditions were applied. The governing equations had been solved using a separate, implicit scheme. The convective terms in momentum and turbulence equations were addressed using a second order upwind technique. The pressure term was discretized with a second-order scheme, and the pressure and velocity variables were coupled with COUPLE. Residual value was given 10^{-3}. The number of iterations was given 100.

For numerical simplification the inlet blood velocity is assumed to be steady. The inlet velocity for the blood in this simulation was fixed to 0.333 [m/s] for Re 1000. The outlet pressure applied 13333 pascals. The outer wall of the fluid zone was considered to be no-slip condition. Using dynamic mesh, the outer wall was coupled with the artery's inner wall. In the static structure, the boundary conditions of artery wall were applied. Fixed condition at the inlet and outlet surface of the artery wall and fluid solid interface boundary condition was applied at the inner face of the artery wall. The main variables affecting blood to be investigated are- artery walls' tensile stress, shear stress (low shear stress causes atherosclerosis), velocity profile and type of flow (fluctuation and periodically varying flow prevent the cells from aligning and it increases contacts between blood cell and damaged intima), periodic change in pressure and tension (they are relevant in the atherosclerosis development) [21].

Simulation was carried out for part of the cardiac cycle to lessen time consumption and only study time scales of interest.

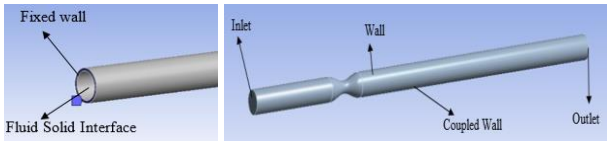

Fig.6 Boundary condition of Artery wall and Fluid Zone

4. Results and Discussion

It is possible to test mesh independency by running several simulations with various mesh resolutions and observing whether outcomes change. Many simulations had been run using different mesh size and the result of maximum velocity and pressure were checked. Here it is seen that the velocity remains identical at the size .5 mm.

Table 4: Variation of elements number and maximum velocity with elements size

Elements	Elements size(mm)	Velocity(max)
70658	1	1.39122
117216	0.8	1.39478
208278	0.6	1.40223
322803	0.5	1.40406
615342	0.4	1.40408
1219458	0.3	1.40401
3560562	0.2	1.40368

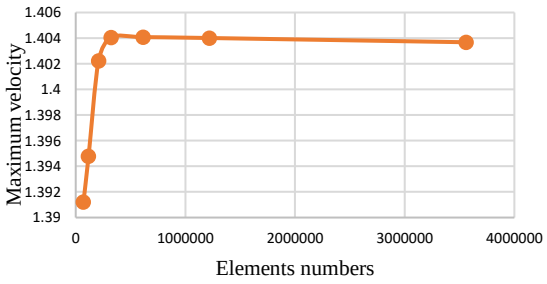

Fig.7 Deviation of velocity with elements numbers

To ensure accuracy of the calculation, the result was compared with Reza Tabe, Farzan Ghalichi [8] result which was valid by the experimental result of Ahmed [21], for same value of Z for the SST K-ω model in case of 50% stenosis

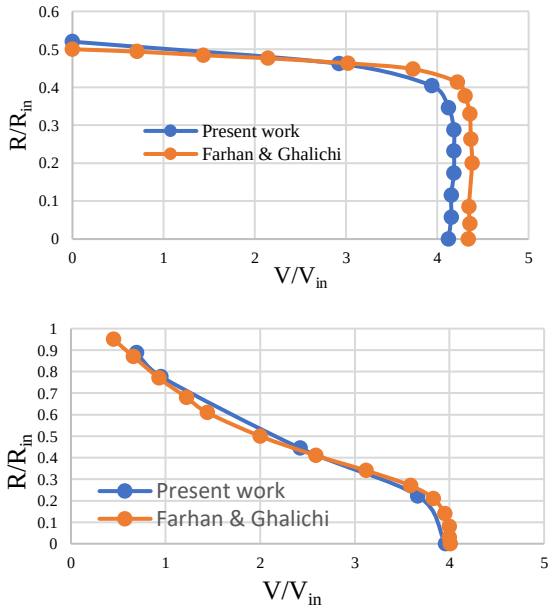

Fig.8 Axial Velocity in the fluid region vs Radial distance (Z=0 and Z=4)

Table 5 Percentages of error with axial distance

X-Axis Location	Percentage of Error (%)
0	3.8
.5	2.9
1	2.7
1.5	1.6
2	1.1
2.5	.6
3	.5
3.5	3.6
4	7.7

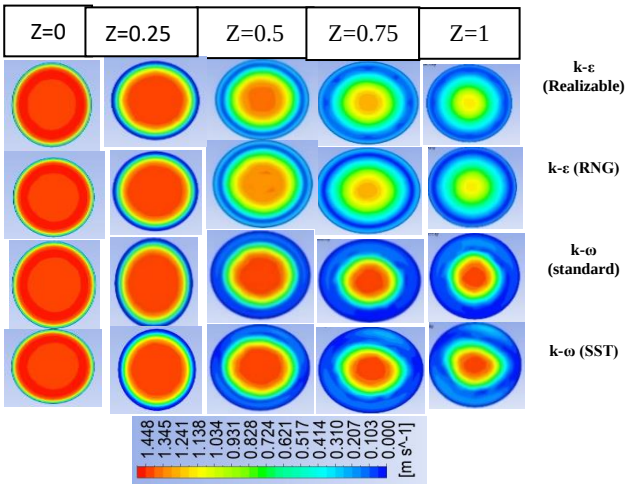

Fig.9 Velocity contour in the cross-section Z=0 Z=.25, Z=.5, Z=.75, Z=1 and Z=2

Velocity contours are shown in different cross-sectional position for the four different turbulence model in figures from **Fig 9** to **Fig 10** At first, the contour is taken in the throat of the stenosis (z=0), where the blood or fluid passing area is the minimum where velocity is maximum in the throat section. and the velocity field from the center to near the wall is almost similar for the four models. At z=0.25, the velocity changes are also same that is the velocity changes between those models starts from z=0.5 section In the k-ϵ realizable and RNG model velocity decrease faster than the K-ω standard and SST model. Due to higher dissipation rate this happens. Later, in the Z=0.75, Z=1, Z=2 section, velocity decreases gradually in all section for the k-ϵ realizable and RNG model as seen in **Fig 10.**

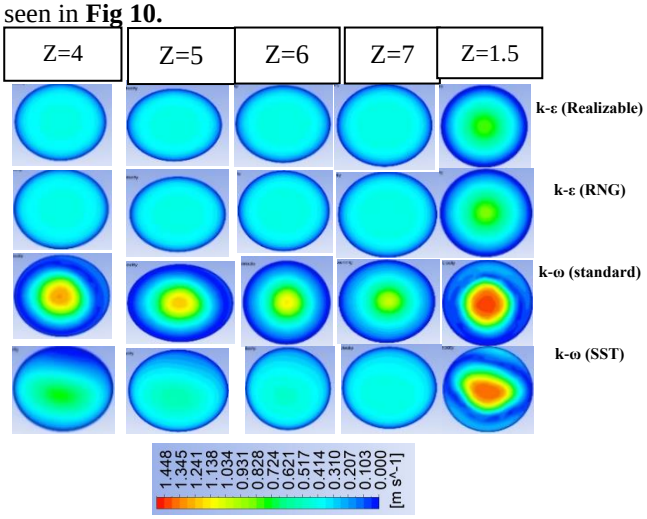

Fig.10 Velocity contour in the cross-section Z=2, Z=3, Z=6, Z=7

Two k-ε models show almost similar results as their damping coefficient value is almost near. Turbulence effect is less visible in those two models. Due to their large dissipation of kinetic energy the velocity decreases so fast. In Z=2 the flow almost loses all its kinetic energy and the flow become fully developed laminar again. Due to this characteristic of fluid flow, eddies formation possibility is less in the both k-ϵ models. In the K-ω standard model velocity remain high longer than the K-ω SST model. Due to this turbulence effect is lengthier in the K-ω standard model than the K-ω SST model. So, the eddies formation capability is more expansive near the wall in K-ω standard model. In the K-ω SST model the wall shear effect is more visible in the velocity. Because of the effect of wall shear, the turbulence kinetic energy is suppressed and the dissipation rate is high near the wall. Due to this, eddy formation is more regular near the stenosed region in K-ω SST model and eddies formation decreases too fast than the K-ω standard model. In the section where Z=8, flow become fully developed except in K-ω Standard model as is evident from **Fig 10**.

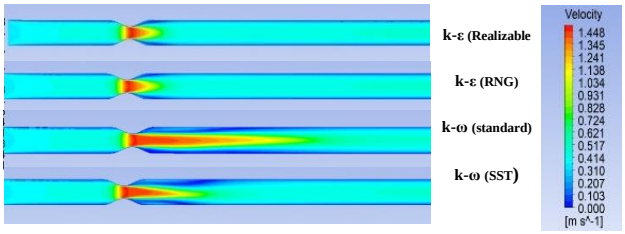

Fig.11 velocity contour in long sectional mid plane for different models

From **Fig.11** In the long section mid plane, comparative velocity fluctuation can be seen more clearly. Here it is seen that the two model of k-ϵ give almost similar effect in the flow field. Turbulence remains too high close to the stenosed region but the eddies formation area is too small. In k-ω standard model eddies size and formation area is more than two models of k-ϵ. But in the k-ω SST model eddies size is high near the stenosed throat but the eddies formation area is less than the K-ω model.

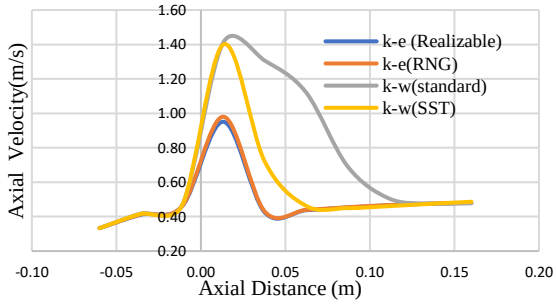

Fig.12 Distance vs velocity graph in the mid plane for four turbulence models

In **Fig.12** it can be seen that in the mid line the velocity is high for the K-ω standard and SST model. Velocity profile is almost same for k-ϵ realizable and RNG models. In the SST model velocity decreases rapidly after the throat. But in the K-ω standard model velocity decreases gradually. The turbulence creation and laminarization

process is very fast in k-ϵ realizable and RNG model. Turbulence affect can be seen better on K-ω standard model. But if we consider the shear affect from the wall, the K-ω SST model gives more preferable result.

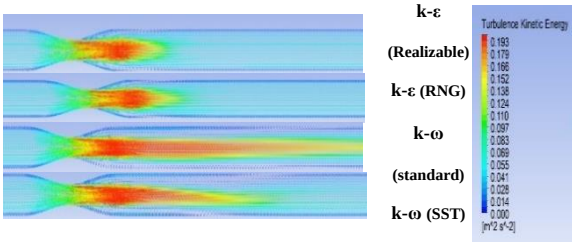

Fig.13 Velocity vector contour for different turbulence models

Fig.13 illustrates that the velocity vector contour for the four-turbulence models. In the k-ϵ models the velocity vector spread out with high velocity. Here the eddies formation area is clear but the area is too small. The velocity decreases too fast than the other two K-ω models. In the K-ω standard contour the velocity remains high for a long range of Z. Here the eddies sizes are low but the formation area is long, vice versa for the SST model. In the **Fig.14** turbulence kinetic energy in the mid plane is shown for all four models. Result is almost same for k-ϵ realizable and RNG model.

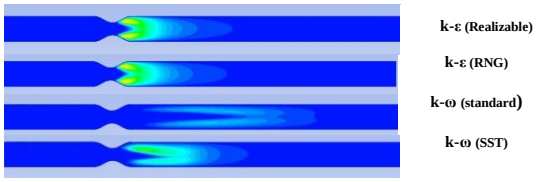

Fig.14 Turbulence kinetic energy (TKE) in mid plane for different models

But due to high dissipation rate the energy decay soon. It is seen in the cross-section plane contour after the Z=2 length the flow velocity decreases and turn into laminar. Eddy forms in between z=.5 to z=2.Due to less effect of wall shear near the wall boundary, the kinetic energy of turbulence is high after the throat region. In the K-ω standard model contour the effect of wall shear is seen more than the k-ϵ model consequently kinetic energy is high far from the throat for the same reason. In the K-ω SST model, the kinetic energy is comparatively higher than the K-ω standard model. Overally the TKE is high in the Z=.75 to Z=5 area. So, according to this, the possibility of next plaque formation is Z=.75 to Z=5 area better shown in the graph in **Fig.16.**

Fig 16 portrays that the eddies size and formation area are clearly seen. In the k-ϵ realizable and RNG model the eddies size and formation areas are too small. Both k-ϵ models show almost similar result. But if we see closely. K-ϵ RNG model streamlines are clearer than the k-ϵ realizable model. From streamline contour of K-ω standard, eddies are formed near the wall. In the void region reverse flow happens.

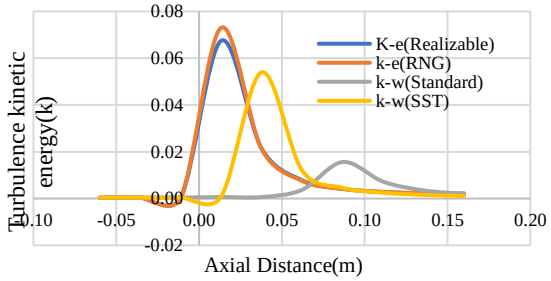

Fig.15 Distance vs turbulence kinetic energy in mid line

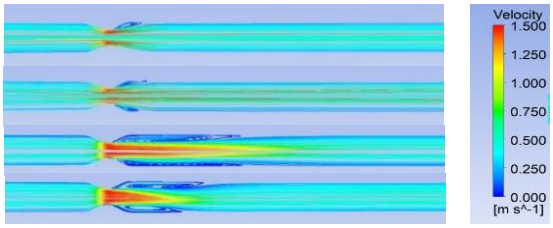

Fig.16 Contour of streamline for different turbulence models

The eddies are smaller in size than the eddies form in K-ω SST model. But the eddies formation area is more than the K-ω SST model. Due to the shear stress transport in SST model, The kinetic energy in the viscous sublayer decreases. For the high dissipation rate near the wall the possibility of eddies formation decreases in SST model. That's why the eddies formation decreases faster in SST model than the K-ω standard model.

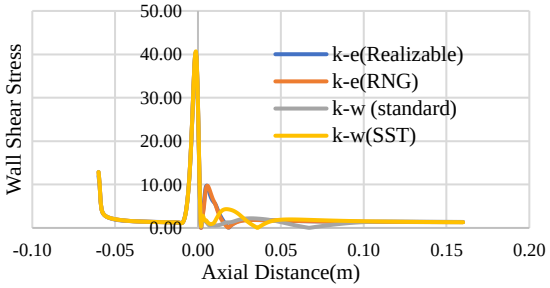

Fig.17 Wall shear stress in wall for different models

In **Fig.17** of wall shear, it is seen that the result is same for the k-ϵ realizable and RNG model. The wall shear is also captured less than the other two model. The main difference happens between the other two model of K-ω model. The maximum wall shear created in the wall in the K-ω SST model. After the stenosis, wall shear decreases and again increases due to the turbulence intensity. The section where the turbulence level is high the wall shear also high. In the K-ω standard model the wall shear increases once after the stenosis and then again increases. Due to the high wall shear stress just after the stenosis, the turbulence kinetic energy decreases and the dissipation rate increases. That's why the turbulence is seen far from the stenosis in K-ω standard model.

In the **Fig.18** the pressure shows same for the k-ϵ realizable and RNG model. But in the K-ω model the pressure increases gradually due to the high velocity or the high turbulence kinetic energy. Due to the good shear effect, the dissipation rate in high in SST model near the wall. That's why the velocity increases and then decreases after Z=2 or 0.02 m

.

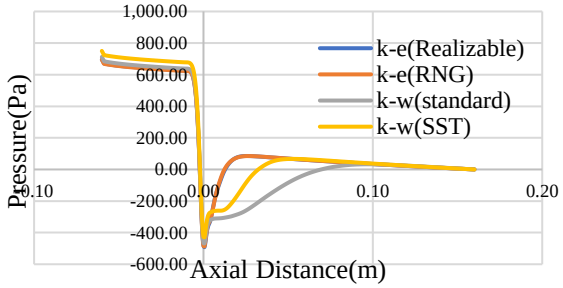

Fig.18: Distance vs pressure in the wall for different models

In the pre-stenosis region, fluid the pressure in the wall is so high. The pressure starts to decrease when the fluid enters into the stenosed region. Due to the rapid increase of fluid velocity in the stenosed region, the pressure mainly decreases. At the throat section, the pressure decreases the most. After passing the throat section the velocity starts to decrease and the pressure starts to increase again. After reaching a certain limit the pressure starts to fall again.

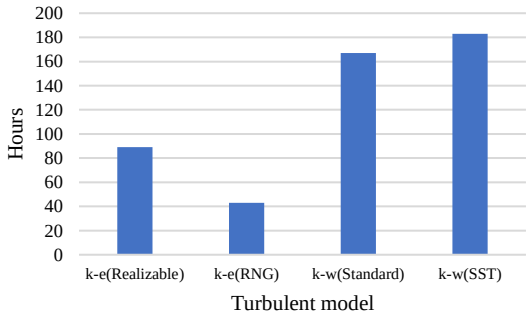

Fig.19: Bar chart of time consumption for different models

In the field of simulation time consumption is a big fact. The convergence time of different turbulent model varies. In the bar chart time consumption is shown for all the four models. The time consumption for the k-ϵ series is less than the K-ω series. As the result of k-ϵ standard and RNG are almost same, the RNG model takes less iteration to solve. In the K-ω model series, the K-ω SST model consume more time and iteration than the K-ω standard model as illustrated in **Fig.19**.

5.Conclusion

The flow field in the vicinity of a stenosis is the focus of the current research. For steady flow, the complicated flow features observed in stenotic flow include flow separation and turbulence.

i. From the velocity comparison, it is seen that the K-ω SST model gives more preferable result than the other model
ii. In the streamline comparison, the eddies creation is seen better on the K-ω Standard model.
iii. In the pressure comparison, on average the K-ω SST gives better result than the other model.
iv. In the wall shear comparison, the maximum shear and the shear variation in wall is seen better in the K-ω SST model
v. According to the time consumption comparison, the K-ω model series more time than the k-ϵ series. In between then the k-ϵ SST model is the most time consumption model.

It can be stipulated from the overall discussion; we can get to a conclusion that the K-ω SST model gives better prediction of wall shear effect than other model though it is more time consuming and is better in most use case scenario. But the ideal model depends on specific patient artery conditions Further research while taking into account the comparison with other turbulence model such as BICGSTAB, DES, LES will enrich the study more. Reynolds number can be varied to see the other effect of blood flow while considering it as non-Newtonian fluid.

Non-linear elastic properties of wall will give more realistic result. As well as Pulsatile flow of blood might give more insight into the nature of such flows.

8. References

[1] Ibrahim Mustafa, Shagufta Ishtiaque, X.Y. Xu and N.B. Wood; Turbulence Modeling in Carotid Stenosed Arteries Using CFD, Department of Chemical Engineering and Technology, Imperial College, London, UK

[2] Reza Tabe, Farzan Ghalichi, Siamak Hossainpour and Kamran Ghasemzadeh; Laminar-to-turbulence and re-laminarization zones detection by simulation of low Reynolds number turbulent blood flow in large stenosed arteries, Bio-Medical Materials and Engineering 27 (2016) 119–129 119, DOI 10.3233/BME-161574

[3] Farzan Ghalichi, Xiaoyan Deng, Alain De Champlain, Yvan Douville, Martin King, and Robert Guidoin; Low Reynolds number turbulence modeling of blood flow in arterial stenoses,13 November 1998, Biorheology 35:4,5 (1998) 281–294

[4] Laxman Kallekar, Chinthapenta Viswanath, and Mohan Anand; Effect of Wall Flexibility on the Deformation during Flow in a Stenosed Coronary Artery, 11 April 2017; Published: 15 April 2017, MDPI

[5] Khairuzzaman Mamun, Mohammad Matiur Rahman1, Most. Nasrin Akhter, and Mohammad Ali, Physiological Non-Newtonian Blood Flow through Single Stenosed Artery, AIP Conference Proceedings 1754, 040001 (2016); doi: 10.1063/1.4958361

[6] Mehdi Jahangiri, Mohsen Saghafian, Mahmoodreza Sadeghi; Numerical study of hemodynamic parameters in pulsatile turbulent blood flow in flexible artery with Stenosis, The 22st Annual International Conference on Mechanical Engineering-ISME2014 22-24 April, 2014, ISME2014-1250

[7] F.P.P. Tan, G. Soloperto, N.B. Wood, S. Thom, A. Hughes, X.Y. Xu; Advanced Computational Models

for Disturbed and Turbulent Flow in Stenosed Human Carotid Artery Bifurcation, Journal of Biomechanical Engineering FEBRUARY 2007, Vol. 129 / 49

[8] Marwa Selmi, Hafedh Belmabrouk and Abdullah Bajahzar; Numerical Study of the Blood Flow in a Deformable Human Aorta Accepted, 19 March 2019; Published: 22 March 2019, MDPI

[9] F.R. Menter; Influence of freestrem values on K-ω turbulence model predictions, Eloret Institute, Palo Alto, California 94303, AIAA journal, VOl 30, No 6

[10] Tang, D.; Yang, C.; Kobayashi, S.; Ku, D.N.; Generalized finite difference method for 3-D viscous flow in stenotic tubes with large wall deformation and collapse, Appl. Number. Math. 2001, 38, 49–68.

[11] Lee, N.; Xu, T; Modelling of flow and wall behavior in a mildly stenosed tube, Med. Eng. Phys. 2002, 24, 575–586.

[12] Cheema, T.A.; Park, C.W. Numerical investigation of hyper elastic wall deformation characteristics in a micro-scale stenotic blood vessel, Korea-Aust. Rheol. J. 2013, 25, 121–127.

[13] Das, A.; Paul, A.; Taylor, M.D.; Banerjee, R.K. Pulsatile arterial wall-blood flow interaction with wall pre-stress computed using an inverse algorithm, Biomed. Eng. Online 2015, 14, S1–S18.

[14] Tang, D.; Yang, C.; Zheng, J.;Woodard, P.K.; Saffitz, J.E.; Sicard, G.A.; Pilgram, T.K.; Yuan, C. Quantifying effects of plaque structure and material properties on stress distributions in human atherosclerotic plaques using 3D FSI models, J. Biomech. Eng. 2005, 127, 1185–1194.

[15] Ali Ostadfar, Biofluid Mechanics Principles and Applications, Academic Press (Elsevier),2016

[16] Mehdi Jahangiri, Mohsen Saghafian, and Mahmood Reza Sadeghi; Numerical Study of Turbulent Pulsatile Blood Flow through Stenosed Artery Using Fluid-Solid Interaction; Hindawi Publishing Corporation, Computational and Mathematical Methods in Medicine, Volume 2015, Article ID 515613, 10 pages

[17] SAAD A. AHMED; Pulsatile Poststenotic Flow Studies with Laser Doppler Anemometry, J. Biomechamcs Vol. No. 9. pp 1984) 0021 Printed in Great Britain,1984 Pergamon Press Ltd

[18] F.R. Menter; Two-Equation Eddy-Viscosity Models for Transonic Flows, AIAA Journal, Vol.32, 1994, pp. 1598-160

[19] Bahador Sharifzadeh, Rasool Kalbasi, Mehdi Jahangiri, Davood Toghraie, Arash Karimipour; Computer modeling of pulsatile blood flow in elastic artery using a software program for application in biomedical engineering; 2020 Published by Elsevier B.V.

[20] Deshpande, M.D. And Giddens, D.P.; Turbulence Measurements in a Constricted Tube, Journal of Fluid Mech. Vol. 97 (1), 1980, pp. 65-89.

NOMENCLATURE

G : generation of turbulent kinetic energy, J/m^{3}s
K : turbulent kinetic energy, m^2/
LES : Large Eddy Simulation
Re : Reynolds number, dimensionless
TAWSS : time averaged wall shear stress
U : velocity magnitude in X direction, m/s
WSS : wall shear stress
τ : shear stress, Pa
ε : dissipation rate of turbulent kinetic energy
ω : specific rate of dissipation, s^{-1}